Decadal application of mineral fertilizers alters the molecular composition and origins of organic matter in particulate and mineral-associated fractions

Zhichao Zou[a], Lixiao Ma[a, b], Xiao Wang[a], Ruirui Chen[c], Davey L. Jones[d,e], Roland Bol[d,f], Di Wu[a*], Zhangliu Du[a**]

[a] *Beijing Key Laboratory of Biodiversity and Organic Farming, College of Resources and Environmental Sciences, China Agricultural University, Beijing 100083, China*

[b] *Institute of Environment and Sustainable Development in Agriculture, Chinese Academy of Agricultural Sciences, Beijing, 100081, China*

[c] *State Key Laboratory of Soil and Sustainable Agriculture, Institute of Soil Science, Chinese Academy of Sciences, Nanjing, 10008, China*

[d] *Environment Centre Wales, Bangor University, Gwynedd, LL57 2UW, UK*

[e] *SoilsWest, Centre for Sustainable Farming Systems, Food Futures Institute, Murdoch University, Murdoch WA 6105, Australia*

[f] *Institute of Bio- and Geosciences, Agrosphere (IBG-3), Forschungszentrum Jülich GmbH, 52425 Jülich, Germany*

[*]Corresponding author: Di Wu

College of Resources and Environmental Sciences, China Agricultural University, Beijing 100193, China

Tel: +86-17801580063

E-mail: d.wu@cau.edu.cn

[**]Corresponding author: Zhangliu Du

College of Resources and Environmental Sciences, China Agricultural University, Beijing 100193, China

Tel: +86-18519156018

E-mail: dzl@cau.edu.cn

Abstract

The extent to which the long-term application of mineral fertilizers regulates the quantity, quality, and stability of soil organic matter (SOM) in soil matrices remains unclear. By combining four biomarkers, i.e., free and bound lipids, lignin phenols and amino sugars, we quantified the molecular composition, decomposition and origins of SOM in response to 10-year fertilization (400 kg N ha^{-1} yr^{-1}, 120 kg P ha^{-1} yr^{-1} and 50 kg K ha^{-1} yr^{-1}) in a cropland in North China. We focused on two contrasting fractions: particulate organic matter (POM), and mineral-associated organic matter (MAOM). Fertilization increased soil organic carbon (SOC) by 23% in MAOM, and altered its composition and origins, despite having a limited effect on bulk SOC levels. Fertilization increased plant-derived terpenoids by 46% in POM and long-chain lipids ($\geq C_{20}$) by 116% in MAOM but decreased short-chain lipids ($<C_{20}$) by 54% in the former fraction. Fertilization reduced suberin-derived lipids by 56% in POM and 30% in MAOM but increased lignin-derived phenols by 74% in POM and 31% in MAOM, implying that crop residues were preferentially stabilized via the POM form. Fertilization decreased the contribution of microbial residues to SOC in both the fractions. Overall, mineral fertilizers tended to reduce labile components within POM (e.g., short-chain lipids), leading to the accrual of recalcitrant molecules (e.g., long-chain lipids, cutin-derived lipids, and lignin-derived phenols) in the MAOM fraction. Collectively, our study suggests that mineral fertilizers can increase SOM stability and persistence by modifying their molecular composition and preservation in the mineral-organic associations in a temperate agroecosystem.

Key words: Mineral fertilizers, Soil organic matter, Biomarkers, Mineral-associated organic matter, Particulate organic matter

1. Introduction

Soil organic matter (SOM) is critical to a functioning agroecosystem because of its key role in maintaining soil fertility, promoting water retention, and soil organic carbon (SOC) sequestration (Hoffland et al., 2020; Kopittke et al., 2022). In typical croplands, large inputs of mineral fertilizers increase crop productivity (Cassman and Dobermann, 2022; He et al., 2020), leading to greater amounts of carbon entering the soil via residues, roots and their exudations, consequently regulating SOM turnover (Averill and Waring, 2018; Man et al., 2021). However, our fundamental understanding of the direction and magnitude of SOC stabilization and sequestration in response to nutrient fertilizers remains unclear. Previous studies have reported higher, neutral, and even lower SOC levels due to fertilizer management across natural and human-managed ecosystems (Khan et al., 2007; Crème et al., 2018; Ghosh et al., 2018; He et al., 2018). In intensive agriculture, mineral fertilizers have been the key strategy to increase and/or maintain crop yields and potential SOC sequestration (Amelung et al., 2020). The observed nutrient-induced changes in SOC accrual have been related to i) the higher plant carbon input via increased litter and rhizodeposition (He et al., 2018; Singh and Benbi, 2018), ii) suppressed microbial metabolism and/or microbial biomass (Boot et al., 2016) and alteration in microbial community structure (Zhang et al., 2018; Ge et al., 2021; Brown et al., 2022). Furthermore, mineral fertilizer inputs may modify SOM formation and stabilization via plant inputs, allocation pathways, and decomposition (Chenu et al., 2019; Song et al., 2019), thus altering its molecular composition and origins. Alongside the contrasting results on how fertilization

115 influences SOC stocks, little information is available about how the application of
116 mineral fertilizers affects the quality of SOM (e.g., molecules, lability, and sources).
117 Investigating the molecular composition of SOM helps uncover its origin and
118 degradation pathway, and thus, an assessment of its lability and stability (Angst et al.,
119 2021). An emerging view is that SOM represents a continuum of progressively
120 decomposing organic compounds with various stages of biogeochemical oxidation
121 (Lehmann and Kleber, 2015). This complex mixture is composed of biomolecules, such
122 as polysaccharides, lipids, lignin, cutin, suberin, and amino sugars (Kögel-Knabner,
123 2002). Biomarker approaches have been shown to be a powerful tool for profiling SOM
124 (Amelung et al., 2008; Gao et al., 2021; Ma et al., 2022a). For example, amino sugars
125 and lignin phenol biomarkers have been used as distinct reporters of microbial- and
126 plant-derived biomolecules (Thevenot et al., 2010; Joergensen, 2018; Liang et al.,
127 2019). Moreover, long-chain free lipids ($\geq C_{20}$) and steroids are believed to be plant-
128 derived, whereas short-chain lipids ($<C_{20}$) and simple carbohydrates (e.g., trehalose)
129 mainly originate from microbes (Bergen et al., 1998; Otto et al., 2005). Bound lipids,
130 such as cutin and suberin, are plant-characterized biomacromolecules used to trace
131 inputs from leaves and roots, respectively (Nierop et al., 2003; Otto and Simpson,
132 2006b; Hamer et al., 2012). However, most studies have focused on the effect of
133 nutrition input (mostly nitrogen, N) in natural systems and found N input could altere
134 these SOM components and origins in grasslands (Creme et al., 2017; Crème et al.,
135 2018) and forest ecosystems (Feng et al., 2010; Vandenenden et al., 2018; Wang et al.,
136 2019; Vandenenden et al., 2021). For instance, long-term N fertilization increased

plant-derived lipids (e.g., steroids, cutin, and suberin) and lignin phenols in a temperate forest (Wang et al., 2019; Vandenenden et al., 2021) and grasslands (Crème et al., 2018). However, uncertainties remain as certain components, such as microbial residues, show inconsistent responses to fertilization (Liang and Balser, 2012; Zhang et al., 2016; Fan et al., 2020). Presumably, these varied results may be attributed to differences in fertilizer type, addition rate, duration, soil type, ecosystem and climate regions (Treseder, 2008; Zhang et al., 2016; Ma et al., 2021; Hu et al., 2022; Ma et al., 2022b). However, few studies have investigated the molecular composition, origins, and stabilization of SOM in response to fertilization in cropland soils which is vital given their greater fertilizers inputs, higher rates of disturbances, lower SOC levels, and growing obligations to store more carbon in these soils to mitigate climate change.

Based on a simple persistence framework, SOM can generally be fractionated into particulate organic matter (POM) and mineral-associated organic matter (MAOM) (Cotrufo et al., 2019; Samson et al., 2020). These two operational fractions are fundamentally distinct in term of their formation, persistence, and functioning (Lavallee et al., 2020; Witzgall et al., 2021). POM is inextricably linked to soil structure development and SOM stabilization (Six and Paustian, 2014), which mainly consists of relatively undecomposed plant fragments (Cotrufo et al., 2015). In contrast, partly decomposed POM can progressively transform into microbial by-products and absorb onto the soil mineral surfaces to form MAOM, which represents the core of stable SOC (Liang et al., 2017; Hemingway et al., 2019; Sokol et al., 2019). MAOM mostly constitutes microbial-derived compounds (Ludwig et al., 2015) or equal plant- and

microbial-derived biomolecules (Angst et al., 2021). These differences in function highlight the need to quantify and characterize POM and MAOM separately (Lavallee et al., 2020). Increasing evidences have shown that soil and crop management practices can alter the amount and synthetic composition of SOM in these functional fractions (Chassé et al., 2021; Kauer et al., 2021; Zhang et al., 2022).

To the best of our knowledge, no study to date has specifically reported the response of SOM molecular composition and origins to long-term application of mineral fertilizer in POM and MAOM fractions in cropland soils. In the present study, we combined several key molecular-level biomarker techniques (e.g., free lipids, bound lipids, lignin-derived phenols, and amino sugars) to investigate the effect of decadal mineral fertilizers addition on the fate, degradation, and origins (e.g., plant- and microbial-derived) of functional POM and MAOM fractions from a temperate agroecosystem in North China. We hypothesized that: 1) mineral fertilizer application would increase the amount of SOM and lignin-derived phenols, while decreasing microbial residues, because of stimulated microbial necromass decay; and 2) nutrient-induced changes in SOM composition and origins would differ between POM and MAOM fractions, where POM would enrich plant-derived SOM, whereas MAOM would accumulate microbial residue.

2. Materials and methods

2.1 Site description, experimental design and soil sampling

A long-term field experiment was conducted at the Huantai Agroecosystem Experiment Station of China Agricultural University (117°58′E, 36°57′N), North China.

The field site has a typical temperate continental monsoon climate with cold winters and hot summers. The mean annual temperature is approximately 12℃ and the mean annual precipitation is 540 mm, with most precipitation occurring from June to August. The dominant double-crop systems are winter wheat (early October to early June) and summer corn (middle June to late September). The tested soil was classified as an aquic inceptisol (a calcareous, fluvo-aquic sandy loam).

The field experiment, established in July 2009, was laid out as a randomized block design with four treatments (three replicates, each 9m × 9m), two of which were chosen for the present study. The two treatments included an unfertilized control and mineral fertilizers application. In the fertilized plot, urea was applied at a total rate of 400 kg N ha^{-1} y^{-1}. Half of the urea was applied as a base fertilizer and the other half was topdressing. Specifically, urea was applied at a rate of 100 kg N ha^{-1} during the wheat sowing (October) and shooting (April) stages. The same rate was applied during the corn sowing (June) and growing season (August). In each fertilization plot, superphosphate was applied at 120 kg P ha^{-1} y^{-1} and potassium sulfate was applied at 50 kg K ha^{-1} y^{-1} when wheat was sown in October. The plots were flooded with water 100 mm per time.

Using a hand auger (with a diameter of 5 cm), soil cores (0–10 cm depth) were randomly collected at three locations from each plot in September 2019 and bulked to obtain a composite sample. This process was repeated for every plot. Subsequently, all soil samples were sieved (< 2 mm) and visible stones and organic materials (e.g., fine roots) were removed before dividing each sample into two portions. One portion was air-dried for the determination of soil physicochemical properties, and another portion was freeze-dried for physical fractionation and further biomarker analysis. After

removing inorganic carbon with diluted HCl (0.5 mol L^{-1}), the SOC and total nitrogen (TN) concentrations were determined using an elemental analyzer (vario MACRO cube, Germany).

Soil fractionation involves dispersing soil samples using low-energy sonication and separating the samples by wet sieving to obtain the POM and MAOM fractions (Christensen, 1992). Briefly, freeze-dried soil (50 g) was placed in a 500 mL beaker, and 250 mL of deionized water was added (soil/water ratio:5:1). The samples were dispersed in 270 J mL^{-1} for 15 min using an ultrasonic generator (SCIENTZ JY92-IIN, Ningbo, China). The suspension was passed through a 53-μm sieve to obtain these two contrasting fractions.

2.2 Targeted compounds identification and quantification

SOM biomarkers were extracted using a series of sequential chemical extractions (Feng and Simpson, 2008). Freeze-dried soil samples were sonicated with organic solvents to extract free lipids, including *n*-alkanes, *n*-alkanols, *n*-alkanoic acids, and steroids. After solvent extraction, the soil residues were subjected to base hydrolysis to obtain bound lipids, which contained suberin-derived compounds (e.g., *ω*-hydroxy and dioic acids) and cutin-derived compounds (e.g., $C_{14\text{-}18}$ hydroxy- and epoxy acids). The remaining subsamples were air-dried and oxidized with CuO to release lignin-derived monomers, namely, vanillyl (V), syringyl (S), and cinnamyl (C) compounds. Amino sugars were separated by HCl hydrolysis (Zhang and Amelung, 1996), including glucosamine (GluN), galactosamine (GalN), muramic acid (MurN), and mannosamine

(ManN). After a successive series of extraction and chemical degradation procedures, the extracts were converted to trimethylsilyl and aldononitrile derivatives, respectively. The derivatized total extracts were analyzed using a gas chromatograph (GC; Agilent 7890B; Agilent Technologies, Santa Clara, CA, USA, USA) equipped with a mass spectrometer (MS; Agilent 5977B, Agilent Technologies). The concentrations of individual extractable compounds were calculated by comparing their peak areas with those of the standards in the total ion current and then normalized to the mass of extracted soil. The detailed extraction procedures and quantification methods were provided in the Supplementary Material.

2.3 Biomarker parameters and calculations

Several molecular indicators have been used to assess the source and degradation stages of SOM at the molecular level. For example, free lipids (primarily *n*-alkanes, *n*-alkanols, and *n*-alkanoic acids) can be categorized into two clusters by their carbon atom numbers: short-chain ($<C_{20}$) and long-chain ($\geq C_{20}$) lipids. Plant-derived lipids include long-chain lipids and steroids, whereas microbial-derived SOM include short-chain lipids and trehalose (Otto et al., 2005; Amelung et al., 2008). Molecular proxies were used to reflect the degradation status of aliphatic lipids by assessing their carbon chain characteristics, such as the average chain length of *n*-alkanes (ACL_{Alk}), *n*-alkanoic acids (ACL_{Fa}), odd-over-even predominance values of *n*-alkanes (OEP) and even-over-odd predominance of *n*-alkanoic acids (EOP) (i.e., higher ACL values correspond to higher degradation) (Otto et al., 2005; Wiesenberg et al., 2010).

The decomposition of cutin-derived lipids was assessed by the ratio of C_{16} or C_{18} ω-hydroxy-alkanoic acids to all hydrolysable C_{16} or C_{18} aliphatic lipids (ω-C_{16}/ΣC_{16} and ω-C_{18}/ΣC_{18}). Both parameters have been reported to increase with progressing cutin degradation (Otto and Simpson, 2006b; Feng and Simpson, 2007). Moreover, the ratio of mid-chain-substituted hydroxy and epoxy acids to total cutin-and suberin-derived compounds (Σmid/ΣS∧C) was calculated to reflect the degradation stage of suberin- and cutin-derived compounds. A decrease in this ratio implied progressive degradation of bound lipids (Otto and Simpson, 2006b). Detailed calculation information is provided in the Supplementary Material.

Lignin degradation was reflected by the acid/aldehyde (Ad/Al) ratios of the V and S units, which have been reported to increase with the progressive oxidation of lignin (Otto and Simpson, 2006a). According to the release efficiency in three types of lignin monomers, the plant-derived carbon in SOC was estimated using the following equation (Yang et al., 2022):

$$P = \frac{\frac{V}{33.3\%} + \frac{S}{90\%} + C}{10\% \times SOC} \times 100\% \quad (1)$$

where V, S, and C represent the lignin phenol monomers (g kg^{-1}), 10% denotes the general lignin content in the main crops residues (Burgess et al., 2002).

Given that the average conversion values from MurN to bacterial carbon are 45 and GluN to fungal carbon are 9, contributions of microbial residual carbon (MRC) to SOC were calculated based on amino sugar data as follows (Appuhn and Joergensen, 2006; Joergensen, 2018):

$$\text{Bacterial residual C} = 45 \times \text{MurN} \quad (2)$$

269 $$\text{Fungal residual C} = (\text{GluN}/179.2 - 2 \times \text{MurN}/251.2) \times 179.2 \times 9 \quad (3)$$

270 where 179.2 and 251.2 are the molecular weights of glucosamine and muramic
271 acid, respectively. The total MRC was estimated as the sum of the fungal and bacterial
272 residual carbon.

273 *2.4 Statistical analyses*

274 Data are presented as the mean values and standard errors (n = 3). The significant
275 differences between treatments and between fractions within a treatment were tested
276 using independent two-sample t-test at $p < 0.05$ (SPSS v21.0 software). A principal
277 component analysis (PCA) was performed to evaluate the changes in SOM profiling
278 (molecular composition, source, and degradation) between treatments and fractions
279 (OriginPro 2020 software; OriginLab, Northampton, MA, USA).

280 **3. Results**

281 *3.1 SOC and TN in bulk soil and fractions*

282 In the non-fertilized treatment, SOC concentrations were 10.2, 3.2, and 12.8 g kg^{-1}
283 in the bulk soil, MAOM, and POM, respectively. After 10 years of fertilization, the
284 SOC concentrations in the fertilized treatment were 11.9, 4.3, and 13.8 g kg^{-1} in the bulk
285 soil, MAOM, and POM fractions, respectively (Table S1). The MAOM fraction
286 dominated the size distribution (>60% of the total recovered mass), and fertilization
287 increased the MAOM mass by 14% (Fig. 1a). Mineral fertilizer addition altered the
288 SOC amounts (g C kg^{-1} bulk soil) stored in the POM and MAOM fractions, with the
289 majority of SOC being concentrated in the MAOM fraction (approximately 90%).

290 Specifically, fertilization increased the amount of SOC by 25% in the MAOM fraction
291 relative to that in control (Fig. 1b). Fertilization increased the TN concentration in POM
292 by 64% relative to the unfertilized control and decreased the carbon/nitrogen ratio in
293 MAOM and bulk soil (Table S1).

294 *3.2 Free lipids compounds in the POM and MAOM fractions*

295 The free lipids identified in the POM and MAOM fractions and bulk soils are
296 shown in Figure 2. For the POM fraction, fertilization decreased the concentrations of
297 short-chain *n*-alkanes and *n*-alkanols by 50% and 57%, respectively, but increased
298 plant-derived terpenoids (e.g., campesterol, stigmasterol, and sitosterol) by 46.4%
299 (Table 1; Fig. 2). Fertilization increased the concentrations of long-chain ($\geq C_{20}$)
300 aliphatic lipids (*n*-alkanes by 93%, *n*-alkanols by 156%, and *n*-alkanoic acids by 161%)
301 in the MAOM fraction, but decreased short-chain ($<C_{20}$) *n*-alkanes and *n*-alkanols by
302 50% and 57%, respectively (Table 1). Several molecular indicators were used to assess
303 the source and degradation status of the free lipids (Fig S1). Overall, ACL_{Alk} and ACL_{Fa}
304 ranged from 26.4–27.7 and 16.6–16.9, respectively, across the fractions and treatments
305 (Fig. S1a and c). Compared with the control, the fertilization treatment had a higher
306 ACL_{Alk} in the POM fraction ($p < 0.01$) than in the MAOM fraction (Fig. S1a). Moreover,
307 mineral fertilizer application increased the OEP and EOP in the POM fraction (Fig. S1b
308 and d; $p < 0.001$).

309 *3.3 Bound lipids in the POM and MAOM fractions*

310 Mineral fertilizer application decreased the suberin-derived lipid concentration by

52% in the POM fraction and 30% in the MAOM fraction (Table 1; $p < 0.05$), whereas fertilization did not affect the cutin-derived constituents in both POM and MAOM fractions. The summed cutin- and/or suberin-derived lipids ($\Sigma S\vee C$; $\Sigma S\wedge C$) were relatively lower under fertilization than the control in the POM fraction rather than the MAOM fraction (Table 1). The addition of mineral fertilizer significantly decreased the suberin/cutin ratio in the POM fraction (Fig. S2a; $p < 0.05$). The ω-$C_{18}/\Sigma C_{18}$ ratio in the POM fraction was higher in the fertilized treatment than that in the control treatment (Fig. S2b; $p < 0.05$). The ω-$C_{16}/\Sigma C_{16}$ ratio in the POM fraction was lower in response to mineral fertilizer addition that in the unfertilized control (Fig. S2c). In addition, fertilization resulted in a higher $\Sigma mid/\Sigma S\wedge C$ ratio than the control in the POM fraction (Fig. S2d).

3.4 Lignin-derived phenols in the POM and MAOM fractions

Mineral fertilizer application increased the specific and total lignin-derived phenols in both POM and MAOM fractions (Fig. 2; Table 1). Specifically, fertilized (cf. control) treatment increased the total lignin-derived phenol concentrations by 74% and 31% in the POM and MAOM fractions, respectively (Fig. 2; Table 1). The lignin oxidation ratios, expressed as $(Ad/Al)_V$ and $(Ad/Al)_S$, were similar between the two fertilizer regimes in both the POM and MAOM fractions (Fig. S3). However, the POM fraction had a higher $(Ad/Al)_V$ value than the MAOM fraction within specific treatment, whereas the reverse trend was found for the $(Ad/Al)_S$ ratio between the POM and MAOM fractions (Fig. S3).

3.5 Amino sugars and microbial necromass in the POM and MAOM fractions

Mineral fertilizers application altered the specific amino sugars (e.g., glucosamine, mannosamine, galactosamine, and muramic acid) between the soil fractions (Fig 2; Table 1). Fertilization reduced some specific amino sugars (except mannosamine) and total amino sugars by 31–37% ($p < 0.05$), whereas the changes in these specific and total amino sugars were not significant in the MAOM fraction. The changes in fungal and bacterial MRC in both the POM and MAOM fractions were significant (Fig. 3). Specifically, mineral fertilizer application decreased bacterial MRC by 37% in the POM fraction, whereas MRC in the MAOM fraction was not significantly different between the treatments. The mineral fertilizer treatment resulted in a higher bacterial MRC in the MAOM than in the POM fraction (Fig. 3a). Similarly, a higher fungal MRC was observed in the MAOM fraction than in the POM fraction across treatments, despite insignificant changes between treatments (Fig. 3b). Fertilization decreased the bacterial-to-fungal MRC ratio (B/F) in the POM fraction rather than in the MAOM fraction (Fig. 3c), whereas this ratio was higher in POM than MAOM fraction across the treatments. However, fertilization decreased the contributions of bacterial MRC to SOC in the POM fraction relative to the control (Fig. 3 d), and similar trend was observed in the contributions of fungal MRC and total MRC to SOC in the MAOM fraction (Fig. 3 d–f). Across treatments, the POM fraction had higher ratios of bacterial MRC, fungal MRC and total MRC to SOC than did the MAOM fraction.

3.6 SOM compounds and proxies in the POM and MAOM fractions

Using the molecular components and related proxies analyzed above, changes in SOM status with fertilization in the POM and MAOM fractions were evaluated using principal component analysis (Fig. 4). The resultant principal components (PCs) explained 78.7% of the variance, and both treatments were separated from one another along PC1, whereas both fractions were separated from one another along PC2 (Fig. 4). B/F, $(Ad/Al)_V$, ω-$C_{18}/\Sigma C_{18}$, and ACL_{Fa} had higher negative loading scores, while EOP, ACL_{Fa}, ω-$C_{16}/\Sigma C_{16}$, ω-$C_{18}/\Sigma C_{18}$, and suberin/cutin had higher positive loading scores along PC1. Control treatment was distinguished by ω-$C_{16}/\Sigma C_{16}$, ω-$C_{18}/\Sigma C_{18}$, and B/F, whereas fertilized treatment was distinguished by $\Sigma mid/\Sigma S \wedge C$ and ACL_{Alk} in the POM fraction. In contrast, in the MAOM fraction, control treatment was shaped by total amino sugars (AS), bacterial MRC, and total bound lipids, whereas fertilized treatment was shaped by total lignin-derived phenols (VSC), total free lipids, EOP, and OEP. The resultant PCs explained 74.6% and 66.1% of the variance in the POM and MAOM fractions, respectively (Fig. S4). After decadal fertilization, the contribution of plant-derived carbon to SOC increased from 38% to 52% in POM and from 17% to 21% in MAOM, whereas the contribution of microbial-derived carbon to SOC decreased from 54% to 38% in POM and 11% to 9% in MAOM (Fig. 5).

4. Discussion

4.1 Effect of mineral fertilizers on SOM origins in the POM and MAOM fractions

Overall, our results showed that decadal fertilization significantly altered the

molecular composition and origins of SOC rather than its concentration (Fig 1; Table 1). The lack of significant changes in SOC concentrations with mineral fertilizers may be attributed to the balance between carbon inputs and degradation (Man et al., 2021). This may also be because SOC accrual in response to fertilization needs decades or longer to manifest (Wiesmeier et al., 2019; Xu et al., 2021). Despite similar SOC concentrations in bulk soil, the application of mineral fertilizer elevated the SOC amount by 26% in the MAOM fraction, implying enhanced carbon persistence (Kleber et al., 2015).

We found a higher proportion of plant-derived carbon (29–32% of SOC in bulk soils) and a lower proportion of microbial-derived carbon (13–20% of SOC) (Fig. 5), which is consistent with a previous study using the same methodology (Chen et al., 2021). However, some previous reports have estimated that MRC contributes over 50% to SOC in temperate cropland soil (Liang et al., 2019; Angst et al., 2021; Wang et al., 2021), which is generally higher than that in the current study. This is because soil pH has a negative effect on amino sugars accumulation (Ni et al., 2020), and the alkaline soil conditions in this study (Table S1) may be the reason for the lower contribution of MRC to SOC.

Our results showed that mineral fertilizer application increased the contribution of plant-derived carbon to SOC in bulk soils (32% vs. 29%) but decreased the microbial-derived contribution (13% vs. 20%) (Fig. 5). This may be attributed to higher crop carbon inputs after fertilization (He et al., 2018). Furthermore, fertilization has been shown to weaken microbial anabolism and necromass accumulation (Janssens et al.,

2010). Regarding the fractions, we observed a much higher contribution of plant-derived carbon in the POM than in the MAOM fraction (Fig. 5). This suggests that POM acts as a functional hot-spot where microorganisms can transform the plant-derived carbon into SOM to increase persistence through the formation of organo-mineral associations (i.e., MAOM) (Witzgall et al., 2021). The contribution of microbial residues to SOC in the MAOM fraction was lower than that in the POM fraction, which could be explained by the dilution effects from the incorporation of other SOC components in the MAOM fraction, resulting in higher amounts of SOC than the POM fraction (Fig. 1b). Moreover, PCA further verified that the POM and MAOM fractions differed in their composition (Fig. 4).

4.2 Different response of free lipids, bound lipids, and lignin-derived phenols to mineral fertilizers

Fertilization increased plant-derived steroids in the POM fraction (Fig 2; Table 1), which is in line with previous studies that reported that nitrogen addition selectively preserved steroids from cropland (Man et al., 2021) and forest soils (Wang et al., 2019; Vandenenden et al., 2021). The elevated levels of steroids after fertilization may originate from crop residue input. This coincided with the higher contribution of plant-derived carbon under fertilization in the POM fraction (Fig. 5). Thus, as a characteristic of fresh plant material, higher OEP values in the POM fraction in fertilized soils (Fig. S1b) further supported this inference (Schäfer et al., 2016). When fresh crop residues enter the POM fraction, labile components such as short-chain lipids may be decomposed faster in the fertilized treatment (Miller et al., 2019; Jilling et al., 2020;

Thomas et al., 2021), as evidenced by the higher ACL_{Alk} in the POM fraction under fertilized soils (Fig. S1a). In contrast, fertilization selectively preserved long-chain lipids in the MAOM fraction (Table 1), probably because of their recalcitrance and affinity with mineral surfaces to form mineral-organic associations (Wiesenberg et al., 2010). The inconsistent responses of short- and long-chain aliphatic lipids in the POM and MAOM fractions indicate that mineral fertilizers may stimulate the preferential degradation of specific free lipid components (e.g., $<C_{20}$ *n*-alkanes and *n*-alkanols), leading to the relative enrichment of long-chain lipids in the MAOM fraction (Table 1).

The present study showed that fertilization reduced the suberin-derived compounds relative to the control (Table 1), reflecting lower root-derived carbon accrual in the fertilized soil. This result supports the argument that less crop carbon is allocated to root growth under higher soil nutrient availability (Li et al., 2015). The lower suberin/cutin ratio in the fertilized treatment (Fig S2a) implies that fertilization preferentially promoted aboveground growth relative to belowground (Lu et al., 2011). The reduced ω-$C_{16}/\Sigma C_{16}$ ratio under fertilization in the POM fraction (Fig. S2c) indicated inhibited degradation of cutin-derived compounds under fertilization, which is supported by other study in temperate forest soils (Vandenenden et al., 2021). Interestingly, the application of mineral fertilizers suppressed cutin-derived compounds degradation in POM, but not in the MAOM fraction (Fig. S2), indicating that the POM fraction is more susceptible to nutrient management than the MAOM fraction (Brown et al., 2014; Miller et al., 2019; Jilling et al., 2020; Lavallee et al., 2020).

Mineral fertilizers application increased lignin-derived phenols in both POM and

MAOM fractions (Fig. 2; Table 1), which was likely due to the increasing straw input (Liu et al., 2016). Lignin distribution in soils is the result of input and decomposition processes (Thevenot et al., 2010). In the present study, lignin degradation proxies, as assessed by $(Ad/Al)_V$ and $(Ad/Al)_S$, were not affected by the application of mineral fertilizers (Fig. S3). This further indicated that the elevated lignin-derived phenols resulted from the added crop residue inputs in the cropland. Regarding the soil fractions, MAOM had higher $(Ad/Al)_S$ value than the POM fraction across treatments, indicating higher degradation of S monomers in MAOM (Fig. S3a). However, we observed the opposite pattern for (Ad/Al)v between the POM and MAOM fractions (Fig. S3b). It is likely that V monomers are more recalcitrant than S monomers during decomposition (Hedges et al., 1988; Bahri et al., 2006). Thus, these biomolecules have a higher probability of interacting with mineral surfaces to form mineral-associated complexity and aggregate (Clemente et al., 2012).

4.3 Different response of microbial residues to mineral fertilizers

Mineral fertilizer application significantly decreased the individual and total amino sugars and MRC in both POM and MAOM fractions (Table1; Fig. 3), which is consistent with other reports in cropland (Chen et al., 2020), grassland, and forest ecosystems (Liang and Balser, 2012; Yuan et al., 2020). Lower microbial residues in fertilized treatments indicate that microbes tend to invest less carbon in anabolism during fertilization (Spohn et al., 2016). Microbial necromass accumulates continuously through the formation of microbial biomass and stabilization of its residues and is gradually consumed through mineralization (Schimel and Schaeffer,

2012; Liang et al., 2019). The decreased contribution of microbial residues to SOC may be associated with enhanced microbial necromass decomposition in response to fertilization (Wang et al., 2021). Although amino sugars play a crucial role in SOM formation, they can be utilized as energy sources (e.g., carbon and nitrogen) to feed microbial growth and activities (Wang et al., 2021). Indeed, long-term fertilization caused carbon limitation in soil (Chen et al., 2018), as evidenced by the lower SOC/TN in our study (Table S1), and thus may decompose microbial necromass as energy to compensate for the microbial carbon demand (Cui et al., 2020; Wang et al., 2021). The additional phosphate fertilizer could promote microbial carbon acquisition by increasing the activity of β-N-acetyl-glucosaminidase and thus microbial residues decomposition (Sinsabaugh et al., 2008; Yuan et al., 2020).

Mineral fertilizers application lowered the B/F ratio in the POM fraction (Fig. 3c), implying that bacterial residues had a relatively faster turnover rate than fungal residues (He et al., 2011). In addition, microbes prefer to use labile substrates enriched in POM form (Cui et al., 2020; Witzgall et al., 2021), resulting in lower bacterial residues due to less protection (Fig. 3a and d). However, bacterial cells can attach directly to clay surfaces non-specifically (Olivelli et al., 2020), which resulted in insignificant differences in bacterial MRC and the contribution of bacterial MRC to SOC within the MAOM fraction. In the present study, higher amino sugars, fungal MRC, and bacterial MRC were observed in the MAOM fraction than in POM (Fig. 3; $p < 0.05$). This is likely because apart from being attached to mineral surfaces, microbial residues may be entrapped in the MAOM fraction, where enzymes are unable to reach (Angst et al.,

2021).

5. Conclusion

The current study found that a 10-year period fertilization altered the molecular composition of SOM rather than its quantity. Furthermore, it provided detailed information on the composition and origins of SOM related to its stabilization and persistence and highlighted the different responses of plant-derived carbon and MRC to mineral fertilizers in the contrasting POM and MAOM fractions. Collectively, the results suggest that mineral fertilizers increase the size of the MAOM-associated carbon pools, by increasing stable components, which enhances SOC sequestration and its persistence in temperate agroecosystems.

Acknowledgements

This study was financially supported by the Natural Science Foundation of China (41671305; 42077037). Zhangliu Du thanks Myrna J. Simpson at the University of Toronto Scarborough for training the biomarker soil extraction and processing. Davey Jones was supported by the UKRI Natural Environment Research Council GCRF project NE/V005871/1.

505 **References**

506 Amelung, W., Bossio, D., de Vries, W., Kögel-Knabner, I., Lehmann, J., Amundson,
507 R., Bol, R., Collins, C., Lal, R., Leifeld, J., 2020. Towards a global-scale soil
508 climate mitigation strategy. Nature Communications 11, 1-10.

509 Amelung, W., Brodowski, S., Sandhage-Hofmann, A., Bol, R., 2008. Combining
510 Biomarker with Stable Isotope Analyses for Assessing the Transformation and
511 Turnover of Soil Organic Matter. Advances in Agronomy 100, 155-250.

512 Angst, G., Mueller, K.E., Nierop, K., Simpson, M.J., 2021. Plant-or microbial-derived?
513 A review on the molecular composition of stabilized soil organic matter. Soil
514 Biology and Biochemistry 156, 108189.

515 Appuhn, A., Joergensen, R.G., 2006. Microbial colonisation of roots as a function of
516 plant species. Soil Biology and Biochemistry 38, 1040-1051.

517 Averill, C., Waring, B., 2018. Nitrogen limitation of decomposition and decay: How
518 can it occur? Global Change Biology 24, 1417-1427.

519 Bahri, H., Dignac, M.F., Rumpel, C., Rasse, D.P., Chenu, C., Mariotti, A., 2006. Lignin
520 turnover kinetics in an agricultural soil is monomer specific. Soil Biology and
521 Biochemistry 38, 1977-1988.

522 Bergen, P., Nott, C.J., Bull, I.D., Poulton, P.R., Evershed, R.P., 1998. Organic
523 geochemical studies of soils from the Rothamsted Classical Experiments - IV.
524 Preliminary results from a study of the effect of soil pH on organic matter decay.
525 Organic Geochemistry 29, 1779-1795.

526 Boot, C.M., Hall, E.K., Denef, K., Baron, J.S., 2016. Long-term reactive nitrogen

loading alters soil carbon and microbial community properties in a subalpine forest ecosystem. Soil Biology and Biochemistry 92, 211-220.

Brown, K.H., Bach, E.M., Drijber, R.A., Hofmockel, K.S., Jeske, E.S., Sawyer, J.E., Castellano, M.J., 2014. A long-term nitrogen fertilizer gradient has little effect on soil organic matter in a high-intensity maize production system. Global Change Biology 20, 1339-1350.

Brown, R.W., Chadwick, D.R., Bending, G.D., Collins, C.D., Whelton, H.L., Daulton, E., Covington, J.A., Bull, I.D., Jones, D.L., 2022. Nutrient (C, N and P) enrichment induces significant changes in the soil metabolite profile and microbial carbon partitioning. Soil Biology and Biochemistry 172, 108779.

Burgess, M., Mehuys, G., Madramootoo, C., 2002. Decomposition of grain-corn residues (Zea mays L.): A litterbag study under three tillage systems. Canadian Journal of Soil Science 82, 127-138.

Cassman, K.G., Dobermann, A., 2022. Nitrogen and the future of agriculture: 20 years on. Ambio 51, 17-24.

Chassé, M., Lutfalla, S., Cecillon, L., Baudin, F., Abiven, S., Chenu, C., Barré, P., 2021. Long-term bare-fallow soil fractions reveal thermo-chemical properties controlling soil organic carbon dynamics. Biogeochemistry 18, 1703-1718.

Chen, H., Li, D., Zhao, J., Zhang, W., Xiao, K., Wang, K., 2018. Nitrogen addition aggravates microbial carbon limitation: Evidence from ecoenzymatic stoichiometry. Geoderma 329, 61-64.

Chen, X., Han, X., Yan, J., Lu, X., Hao, X., Wang, W., Biswas, A., Zhu-Barker, X.,

549 Zou, W., 2020. Land use and mineral fertilization influence soil microbial biomass
550 and residues: A case study of a Chinese Mollisol. European Journal of Soil
551 Biology 100, 103216.
552 Chen, X., Hu, Y., Xia, Y., Zheng, S., Ma, C., Rui, Y., He, H., Huang, D., Zhang, Z.,
553 Ge, T., 2021. Contrasting pathways of carbon sequestration in paddy and upland
554 soils. Global Change Biology 27, 2478-2490.
555 Chenu, C., (Fig. 3c) Angers, D.A., Barré, P., Derrien, D., Arrouays, D., Balesdent, J.,
556 2019. Increasing organic stocks in agricultural soils: Knowledge gaps and
557 potential innovations Soil and Tillage Research 188, 41-52.
558 Christensen, B.T., 1992. Physical fractionation of soil and organic matter in primary
559 particle size and density separates. Advances in soil sciences 20, 1-90.
560 Clemente, J.S., Simpson, A.J., Simpson, M.J., 2012. Association of specific organic
561 matter compounds in size fractions of soils under different environmental controls.
562 Organic Geochemistry 42, 1169-1180.
563 Cotrufo, M.F., Ranalli, M.G., Haddix, M.L., Six, J., Lugato, E., 2019. Soil carbon
564 storage informed by particulate and mineral-associated organic matter. Nature
565 Geoscience 12, 989-994.
566 Cotrufo, M.F., Soong, J.L., Horton, A.J., Campbell, E.E., Haddix, M.L., Wall, D.H.,
567 Parton, W.J., 2015. Formation of soil organic matter via biochemical and physical
568 pathways of litter mass loss. Nature Geoscience 8, 776-779.
569 Creme, A., Chabbi, A., Gastal, F., Rumpel, C., 2017. Biogeochemical nature of
570 grassland soil organic matter under plant communities with two nitrogen sources.

571 Plant and soil 415, 189-201.
572 Crème, A., Rumpel, C., Le Roux, X., Romian, A., Lan, T., Chabbi, A., 2018. Ley
573 grassland under temperate climate had a legacy effect on soil organic matter
574 quantity, biogeochemical signature and microbial activities. Soil Biology and
575 Biochemistry 122, 203-210.
576 Cui, J., Zhu, Z., Xu, X., Liu, S., Jones, D.L., Kuzyakov, Y., Shibistova, O., Wu, J., Ge,
577 T., 2020. Carbon and nitrogen recycling from microbial necromass to cope with
578 C: N stoichiometric imbalance by priming. Soil Biology and Biochemistry 142,
579 107720.
580 Fan, Y., Yang, L., Zhong, X., Yang, Z., Lin, Y., Guo, J., Chen, G., Yang, Y., 2020. N
581 addition increased microbial residual carbon by altering soil P availability and
582 microbial composition in a subtropical Castanopsis forest. Geoderma 375, 114470.
583 Feng, X., Simpson, A.J., Schlesinger, W.H., Simpson, M.J., 2010. Altered microbial
584 community structure and organic matter composition under elevated CO2 and N
585 fertilization in the duke forest. Global Change Biology 16, 2104-2116.
586 Feng, X., Simpson, M.J., 2007. The distribution and degradation of biomarkers in
587 Alberta grassland soil profiles. Organic Geochemistry 38, 1558-1570.
588 Feng, X., Simpson, M.J., 2008. Temperature responses of individual soil organic matter
589 components. Journal of Geophysical Research: Biogeosciences 113.
590 Gao, Q., Ma, L., Fang, Y., Zhang, A., Li, G., Wang, J., Wu, D., Wu, W., Du, Z., 2021.
591 Conservation tillage for 17 years alters the molecular composition of organic
592 matter in soil profile. Science of the Total Environment 762, 143116.

593 Ge, Z., Li, S., Bol, R., Zhu, P., Peng, C., An, T., Cheng, N., Liu, X., Li, T., Xu, Z.,
594 2021. Differential long-term fertilization alters residue-derived labile organic
595 carbon fractions and microbial community during straw residue decomposition.
596 Soil and Tillage Research 213, 105120.
597 Ghosh, A., Bhattacharyya, R., Meena, M., Dwivedi, B., Singh, G., Agnihotri, R.,
598 Sharma, C., 2018. Long-term fertilization effects on soil organic carbon
599 sequestration in an Inceptisol. Soil and Tillage Research 177, 134-144.
600 Hamer, U., Rumpel, C., Dignac, M.F., 2012. Cutin and suberin biomarkers as tracers
601 for the turnover of shoot and root derived organic matter along a chronosequence
602 of Ecuadorian pasture soils. European Journal of Soil Science 63, 808-820.
603 He, H., Zhang, W., Zhang, X., Xie, H., Zhuang, J., 2011. Temporal responses of soil
604 microorganisms to substrate addition as indicated by amino sugar differentiation.
605 Soil Biology and Biochemistry 43, 1155-1161.
606 He, R., Shao, C., Shi, R., Zhang, Z., Zhao, R., 2020. Development trend and driving
607 factors of agricultural chemical fertilizer efficiency in China. Sustainability 12,
608 4607.
609 He, Y., He, X., Xu, M., Zhang, W., Yang, X., Huang, S., 2018. Long-term fertilization
610 increases soil organic carbon and alters its chemical composition in three wheat-
611 maize cropping sites across central and south China. Soil and Tillage Research
612 177, 79-87.
613 Hedges, J.I., Blanchette, R.A., Weliky, K., Devol, A.H., 1988. Effects of fungal
614 degradation on the CuO oxidation products of lignin: a controlled laboratory study.

615 Geochimica Et Cosmochimica Acta 52, 2717-2726.
616 Hemingway, J.D., Rothman, D.H., Grant, K.E., Rosengard, S.Z., Eglinton, T.I., Derry,
617 L.A., Galy, V., 2019. Mineral protection regulates long-term global preservation
618 of natural organic carbon. Nature 570, 228-231.
619 Hoffland, E., Kuyper, T.W., Comans, R.N., Creamer, R.E., 2020. Eco-functionality of
620 organic matter in soils. Plant and soil 455, 1-22.
621 Hu, J., Huang, C., Zhou, S., Liu, X., Dijkstra, F.A., 2022. Nitrogen addition increases
622 microbial necromass in croplands and bacterial necromass in forests: A global
623 meta-analysis. Soil Biology and Biochemistry 165, 108500.
624 Janssens, I., Dieleman, W., Luyssaert, S., Subke, J.-A., Reichstein, M., Ceulemans, R.,
625 Ciais, P., Dolman, A.J., Grace, J., Matteucci, G., 2010. Reduction of forest soil
626 respiration in response to nitrogen deposition. Nature Geoscience 3, 315-322.
627 Jilling, A., Kane, D., Williams, A., Yannarell, A.C., Davis, A., Jordan, N.R., Koide,
628 R.T., Mortensen, D.A., Smith, R.G., Snapp, S.S., 2020. Rapid and distinct
629 responses of particulate and mineral-associated organic nitrogen to conservation
630 tillage and cover crops. Geoderma 359, 114001.
631 Joergensen, R.G., 2018. Amino sugars as specific indices for fungal and bacterial
632 residues in soil. Biology and Fertility of Soils 54, 559-568.
633 Kauer, K., Pärnpuu, S., Talgre, L., Eremeev, V., Luik, A., 2021. Soil Particulate and
634 Mineral-Associated Organic Matter Increases in Organic Farming under Cover
635 Cropping and Manure Addition. Agriculture 11, 903.
636 Khan, S., Mulvaney, R., Ellsworth, T., Boast, C., 2007. The myth of nitrogen

637 fertilization for soil carbon sequestration. Journal of Environmental Quality 36,
638 1821-1832.
639 Kleber, M., Eusterhues, K., Keiluweit, M., Mikutta, C., Mikutta, R., Nico, P.S., 2015.
640 Mineral–organic associations: formation, properties, and relevance in soil
641 environments. Advances in Agronomy 130, 1-140.
642 Kögel-Knabner, I., 2002. The macromolecular organic composition of plant and
643 microbial residues as inputs to soil organic matter. Soil Biology and Biochemistry
644 34, 139-162.
645 Kopittke, P.M., Berhe, A.A., Carrillo, Y., Cavagnaro, T.R., Chen, D., Chen, Q.-L.,
646 Roman Dobarco, M., Dijkstra, F.A., Field, D.J., Grundy, M.J., 2022. Ensuring
647 planetary survival: the centrality of organic carbon in balancing the
648 multifunctional nature of soils. Critical Reviews in Environmental Science
649 Technology 52, 4308-4324.
650 Lavallee, J.M., Soong, J.L., Cotrufo, M.F., 2020. Conceptualizing soil organic matter
651 into particulate and mineral-associated forms to address global change in the 21st
652 century. Global Change Biology 26, 1-13.
653 Lehmann, J., Kleber, M., 2015. The contentious nature of soil organic matter. Nature
654 528, 60-68.
655 Li, W., Jin, C., Guan, D., Wang, Q., Wang, A., Yuan, F., Wu, J., 2015. The effects of
656 simulated nitrogen deposition on plant root traits: a meta-analysis. Soil Biology
657 and Biochemistry 82, 112-118.
658 Liang, C., Amelung, W., Lehmann, J., Kästner, M., 2019. Quantitative assessment of

659 microbial necromass contribution to soil organic matter. Global Change Biology
660 25, 3578-3590.
661 Liang, C., Balser, T.C., 2012. Warming and nitrogen deposition lessen microbial
662 residue contribution to soil carbon pool. Nature Communications 3, 1-4.
663 Liang, C., Schimel, J.P., Jastrow, J.D., 2017. The importance of anabolism in microbial
664 control over soil carbon storage. Nature Microbiology 2, 17105.
665 Liu, J., Wu, N., Wang, H., Sun, J., Peng, B., Jiang, P., Bai, E., 2016. Nitrogen addition
666 affects chemical compositions of plant tissues, litter and soil organic matter.
667 Ecology 97, 1796-1806.
668 Lu, M., Zhou, X., Luo, Y., Yang, Y., Fang, C., Chen, J., Li, B., 2011. Minor stimulation
669 of soil carbon storage by nitrogen addition: a meta-analysis. Agriculture,
670 Ecosystems Environment 140, 234-244.
671 Ludwig, M., Achtenhagen, J., Miltner, A., Eckhardt, K.-U., Leinweber, P., Emmerling,
672 C., Thiele-Bruhn, S., 2015. Microbial contribution to SOM quantity and quality in
673 density fractions of temperate arable soils. Soil Biology and Biochemistry 81, 311-
674 322.
675 Ma, L., Ju, Z., Fang, Y., Vancov, T., Gao, Q., Wu, D., Zhang, A., Wang, Y., Hu, C.,
676 Wu, W., 2022a. Soil warming and nitrogen addition facilitates lignin and
677 microbial residues accrual in temperate agroecosystems. Soil Biology and
678 Biochemistry 170, 108693.
679 Ma, S., Chen, G., Du, E., Tian, D., Xing, A., Shen, H., Ji, C., Zheng, C., Zhu, J., Zhu,
680 J., 2021. Effects of nitrogen addition on microbial residues and their contribution

to soil organic carbon in China's forests from tropical to boreal zone. Environmental Pollution 268, 115941.

Ma, X., Zhang, W., Zhang, X., Bao, X., Xie, H., Li, J., He, H., Liang, C., Zhang, X., 2022b. Dynamics of microbial necromass in response to reduced fertilizer application mediated by crop residue return. Soil Biology and Biochemistry 165, 108512.

Man, M., Deen, B., Dunfield, K.E., Wagner-Riddle, C., Simpson, M.J., 2021. Altered soil organic matter composition and degradation after a decade of nitrogen fertilization in a temperate agroecosystem. Agriculture, ecosystems environmental 310, 107305.

Miller, G., Rees, R., Griffiths, B., Ball, B., Cloy, J., 2019. The sensitivity of soil organic carbon pools to land management varies depending on former tillage practices. Soil and Tillage Research 194, 104299.

Ni, X., Liao, S., Tan, S., Wang, D., Yang, Y., 2020. A quantitative assessment of amino sugars in soil profiles. Soil Biology and Biochemistry 143, 107762.

Nierop, K.G.J., Naafs, D.F.W., Verstraten, J.M., 2003. Occurrence and distribution of ester-bound lipids in Dutch coastal dune soils along a pH gradient. Organic Geochemistry 34, 719-729.

Olivelli, M.S., Fugariu, I., Torres Sanchez, R.M., Curutchet, G., Simpson, A.J., Simpson, M.J., 2020. Unraveling Mechanisms behind Biomass–Clay Interactions Using Comprehensive Multiphase Nuclear Magnetic Resonance (NMR) Spectroscopy. ACS Earth Space Chemistry 4, 2061-2072.

703 Otto, A., Shunthirasingham, C., Simpson, M.J., 2005. A comparison of plant and
704 microbial biomarkers in grassland soils from the Prairie Ecozone of Canada.
705 Organic Geochemistry 36, 425-448.
706 Otto, A., Simpson, M.J., 2006a. Evaluation of CuO oxidation parameters for
707 determining the source and stage of lignin degradation in soil. Biogeochemistry
708 80, 121-142.
709 Otto, A., Simpson, M.J., 2006b. Sources and composition of hydrolysable aliphatic
710 lipids and phenols in soils from western Canada. Organic Geochemistry 37, 385-
711 407.
712 Samson, M.L., Chantigny, M.H., Vanasse, A., Menasseri-Aubry, S., Angers, D.A.,
713 2020. Management practices differently affect particulate and mineral-associated
714 organic matter and their precursors in arable soils. Soil Biology and Biochemistry
715 148, 107867.
716 Schäfer, I.K., Lanny, V., Franke, J., Eglinton, T.I., Zech, M., Vysloužilová, B., Zech,
717 R., 2016. Leaf waxes in litter and topsoils along a European transect. Soil 2, 551-
718 564.
719 Schimel, J.P., Schaeffer, S.M., 2012. Microbial control over carbon cycling in soil.
720 Frontiers in Microbiology 3, 348.
721 Singh, P., Benbi, D.K., 2018. Nutrient management effects on organic carbon pools in
722 a sandy loam soil under rice-wheat cropping. Archives of Agronomy Soil Science
723 64, 1879-1891.
724 Sinsabaugh, R.L., Lauber, C.L., Weintraub, M.N., Ahmed, B., Allison, S.D., Crenshaw,

C., Contosta, A.R., Cusack, D., Frey, S., Gallo, M.E., 2008. Stoichiometry of soil enzyme activity at global scale. Ecology Letters 11, 1252-1264.

Six, J., Paustian, K., 2014. Aggregate-associated soil organic matter as an ecosystem property and a measurement tool. Soil Biology and Biochemistry 68, A4-A9.

Sokol, N.W., Sanderman, J., Bradford, M.A., 2019. Pathways of mineral-associated soil organic matter formation: Integrating the role of plant carbon source, chemistry, and point of entry. Global Change Biology 25, 12-24.

Song, J., Wan, S., Piao, S., Knapp, A.K., Classen, A.T., Vicca, S., Ciais, P., Hovenden, M.J., Leuzinger, S., Beier, C., 2019. A meta-analysis of 1,119 manipulative experiments on terrestrial carbon-cycling responses to global change. Nature Ecology Evolution 3, 1309-1320.

Spohn, M., Pötsch, E.M., Eichorst, S.A., Woebken, D., Wanek, W., Richter, A., 2016. Soil microbial carbon use efficiency and biomass turnover in a long-term fertilization experiment in a temperate grassland. Soil Biology and Biochemistry 97, 168-175.

Thevenot, M., Dignac, M.F., Rumpel, C., 2010. Fate of lignins in soils: A review. Soil Biology and Biochemistry 42, 1200-1211.

Thomas, C.L., Jansen, B., van Loon, E.E., Wiesenberg, G.L., 2021. Transformation of n-alkanes from plant to soil: a review. Soil 7, 785-809.

Treseder, K.K., 2008. Nitrogen additions and microbial biomass: a meta-analysis of ecosystem studies. Ecology Letters 11, 1111-1120.

Vandenenden, L., Anthony, M.A., Frey, S., Simpson, M.J., 2021. Biogeochemical

747 evolution of soil organic matter composition after a decade of warming and
748 nitrogen addition. Biogeochemistry 156, 161-175.
749 Vandenenden, L., Frey, S.D., Nadelhoffer, K.J., Lemoine, J.M., Lajtha, K., Simpson,
750 M.J., 2018. Molecular-level changes in soil organic matter composition after
751 10 years of litter, root and nitrogen manipulation in a temperate forest.
752 Biogeochemistry 141, 183–197.
753 Wang, B., An, S., Liang, C., Liu, Y., Kuzyakov, Y., 2021. Microbial necromass as the
754 source of soil organic carbon in global ecosystems. Soil Biology and Biochemistry
755 162, 108422.
756 Wang, J.J., Bowden, R.D., Lajtha, K., Washko, S.E., Wurzbacher, S.J., Simpson, M.J.,
757 2019. Long-term nitrogen addition suppresses microbial degradation, enhances
758 soil carbon storage, and alters the molecular composition of soil organic matter.
759 Biogeochemistry 142, 299-313.
760 Wiesenberg, G.L.B., Dorodnikov, M., Kuzyakov, Y., 2010. Source determination of
761 lipids in bulk soil and soil density fractions after four years of wheat cropping.
762 Geoderma 156, 267-277.
763 Wiesmeier, M., Urbanski, L., Hobley, E., Lang, B., von Lützow, M., Marin-Spiotta, E.,
764 van Wesemael, B., Rabot, E., Ließ, M., Garcia-Franco, N., 2019. Soil organic
765 carbon storage as a key function of soils-A review of drivers and indicators at
766 various scales. Geoderma 333, 149-162.
767 Witzgall, K., Vidal, A., Schubert, D.I., Höschen, C., Schweizer, S.A., Buegger, F.,
768 Pouteau, V., Chenu, C., Mueller, C.W., 2021. Particulate organic matter as a

functional soil component for persistent soil organic carbon. Nature Communications 12, 1-10.

Xu, C., Xu, X., Ju, C., Chen, H.Y., Wilsey, B.J., Luo, Y., Fan, W., 2021. Long-term, amplified responses of soil organic carbon to nitrogen addition worldwide. Global Change Biology 27, 1170-1180.

Yang, Y., Dou, Y., Wang, B., Wang, Y., Liang, C., An, S., Soromotin, A., Kuzyakov, Y., 2022. Increasing contribution of microbial residues to soil organic carbon in grassland restoration chronosequence. Soil Biology and Biochemistry 170, 108688.

Yuan, Y., Li, Y., Mou, Z., Kuang, L., Liu, Z., 2020. Phosphorus addition decreases microbial residual contribution to soil organic carbon pool in a tropical coastal forest. Global Change Biology 27, 454-466.

Zhang, T.a., Chen, H.Y., Ruan, H., 2018. Global negative effects of nitrogen deposition on soil microbes. ISME 12, 1817-1825.

Zhang, W., Cui, Y., Lu, X., Bai, E., He, H., Xie, H., Liang, C., Zhang, X., 2016. High nitrogen deposition decreases the contribution of fungal residues to soil carbon pools in a tropical forest ecosystem. Soil Biology and Biochemistry 97, 211-214.

Zhang, X., Amelung, W., 1996. Gas chromatographic determination of muramic acid, glucosamine, mannosamine, and galactosamine in soils. Soil Biology and Biochemistry 28, 1201-1206.

Zhang, Z., Kaye, J.P., Bradley, B.A., Amsili, J.P., Suseela, V., 2022. Cover crop functional types differentially alter the content and composition of soil organic

carbon in particulate and mineral-associated fractions. Global Change Biology 28, 5831-5848.

Table 1. Concentrations of soil organic matter (SOM) components in particulate organic matter (POM) and mineral-associated organic matter (MAOM) fractions from a 10-year field experiment in North China Plain where replicated plots received either no fertilizers or mineral fertilizers.

Compounds name	POM		MAOM	
	Control	Fertilization	Control	Fertilization
Solvent-extracted products (μg g^{-1} soil)				
Short-chain *n*-alkanes (<C_{20})	**0.18±0.02***	0.09±0.01	0.55±0.04	0.90±0.23
Long-chain *n*-alkanes (≥C_{20})	2.11±0.31	1.44±0.17	3.92±0.33	**7.55±0.54***
Short-chain *n*-alkanols	**0.21±0.05***	0.09±0.02	0.72±0.04	1.12±0.19
Long-chain *n*-alkanols	1.16±0.14	0.85±0.07	1.11±0.09	**2.84±0.24***
Short-chain *n*-alkanoic acid	17. 8±2.0	17.4±2.3	39.8±2.6	51.5±4.4
Long-chain *n*-alkanoic acid	1.82±0.3	1.29±0.31	1.09±0.06	**2.84±0.48***
Carbohydrate	2.37±0.32	2.14±0.48	2.68±0.14	2.48±0.42
Steroids	1.12±0.15	**2.64±0.21***	2.81±0.15	2.95±0.76
Base hydrolyzed products (μg g^{-1} soil)				
Suberin-derived lipids	**4.30±0.45***	2.08±0.17	**6.07±0.38***	4.25±0.18
Cutin-derived lipids	6.68±1.58	4.83±0.22	10.27±1.06	10.25±1.06
Suberin- or cutin-derived lipids	**8.46±1.69***	4.57±0.3	11.45±0.95	11.87±1.25
Suberin- and cutin-derived lipids	**19.4±3.67***	11.5±0.68	27.8±2.3	26.4±2.1
CuO oxidized products (μg g^{-1} soil)				
Vanillyls	8.85±0.88	**15.76±1.64***	36.65±3.51	**55.4±3.91***
Syringyls	7.00±0.82	**12.00±1.44***	35.06±4.57	48.68±4.35
Cinnamyls	2.19±0.23	**3.67±0.74***	5.2±0.74	**7.99±1.26***
Total lignin-derived phenols	18.0±1.7	**31.4±3.8***	76.9±8.7	**112.1±5.8***
Amino sugars (μg g^{-1} soil)				
Glucosamine	**47.4±0.7***	32.9±5.34	98.5±8.1	95.6±3.8
Mannose	1.41±0.06	1.34±0.15	1.61±0.15	**3.47±0.26***
Galactosamine	**24.4±0.3***	15. 7±2.7	34.8±5.0	29.1±0.3
Muramic acid	**3.12±0.06***	1.98±0.31	4.08±0.37	4.26±0.18
Total amino sugars	**76.3±1.0***	51. 9±8. 4	139.0±13.5	132.5±3.7

Values are presented as means ± SEM (n = 3). Values that are statistically different between control and fertilization treatments are indicated by *p < 0.05. SOM compound concentrations were normalised to bulk soil dry weight (μg g^{-1} soil).

Figure 1

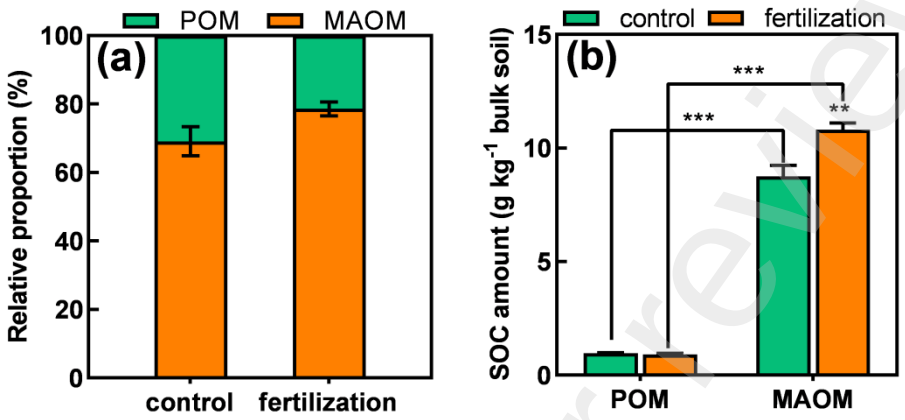

Figure 2

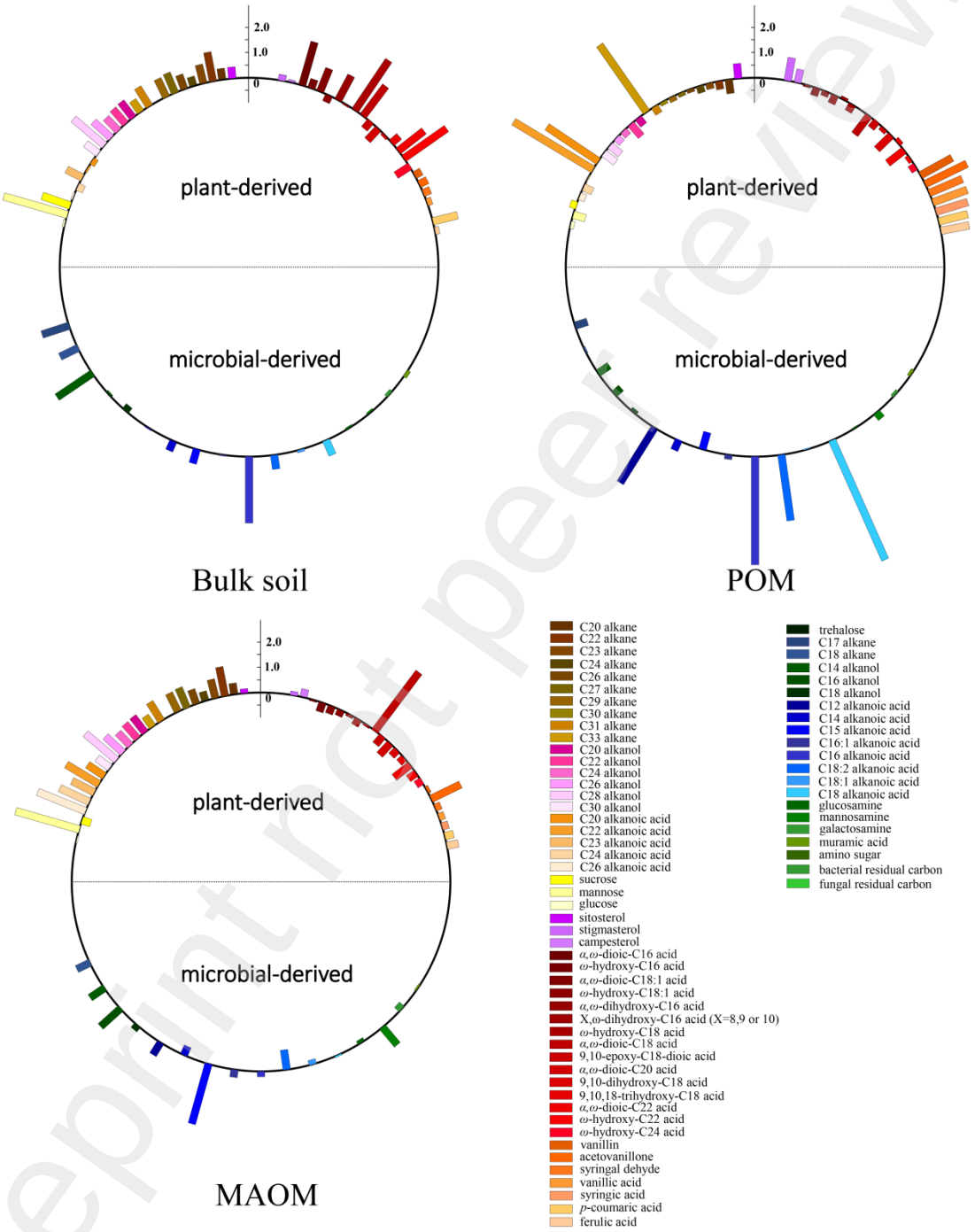

Figure 3

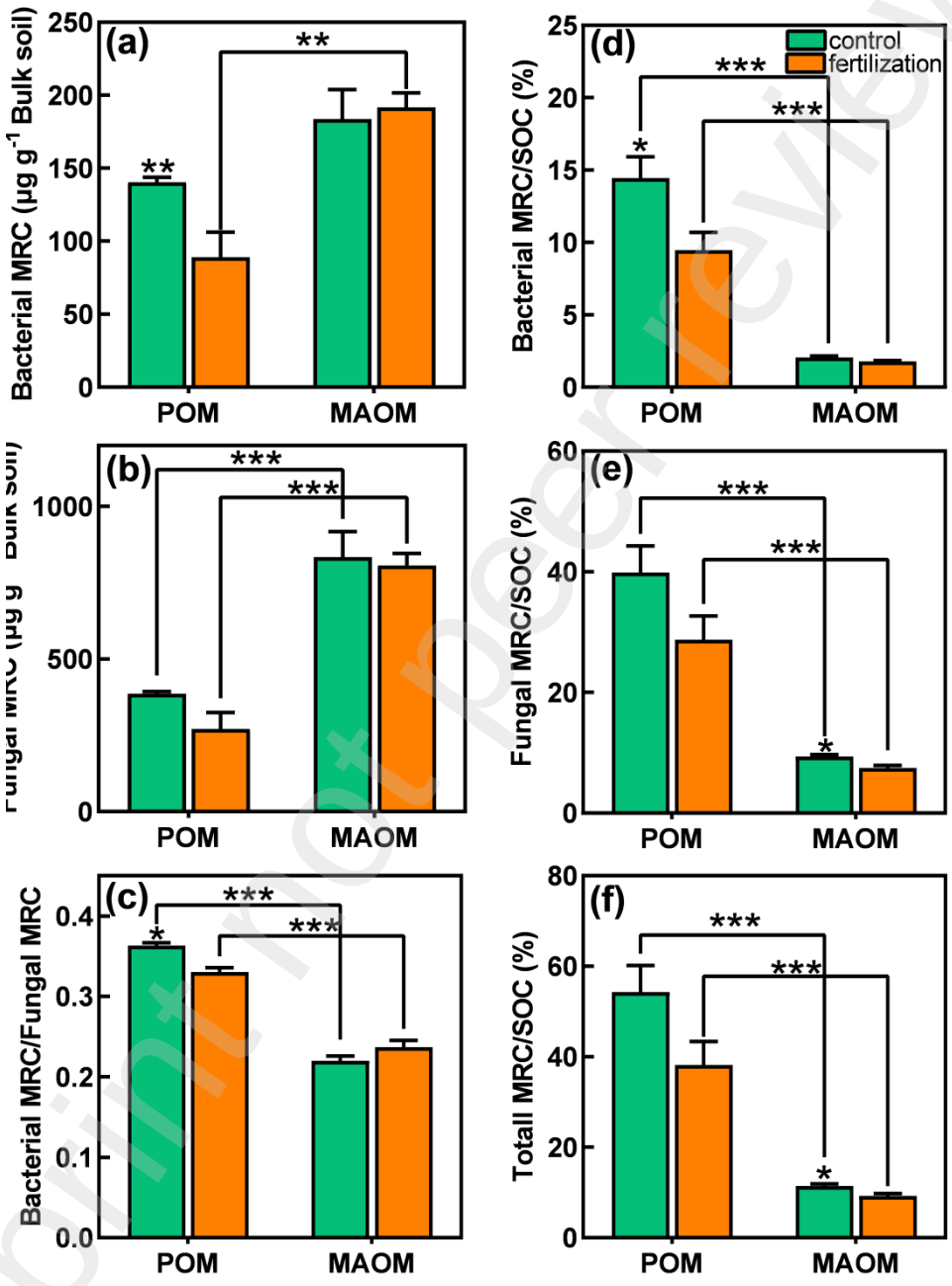

Figure 4

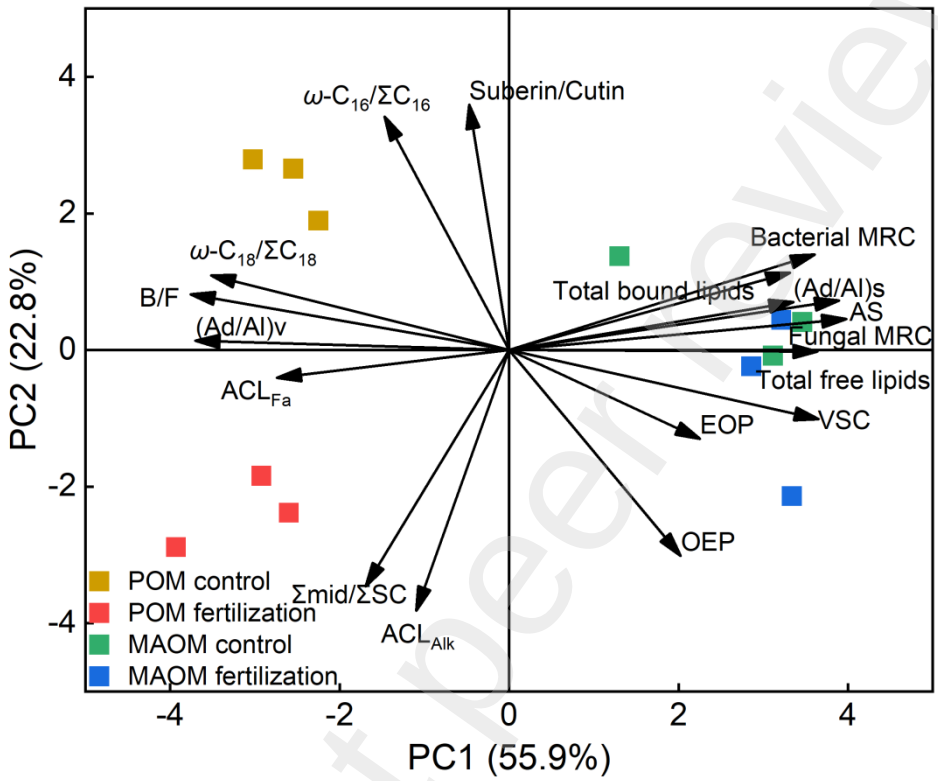

Figure 5

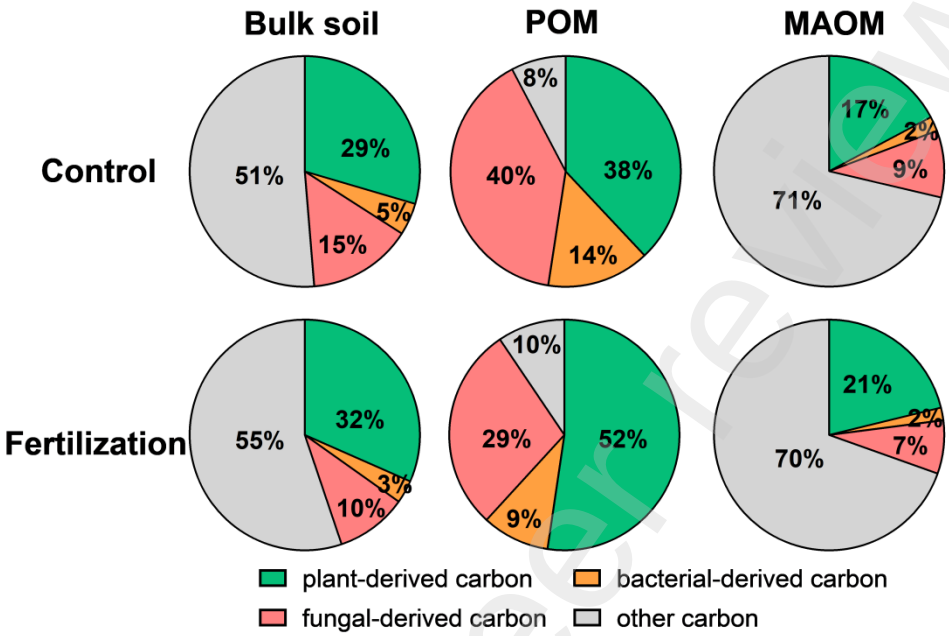

Figure captions:

Fig. 1. Response of fraction mass proportion (a) and soil organic carbon (SOC) amount (b) changes in particulate organic matter (POM) and mineral-associated organic matter (MAOM) fractions as influenced by mineral fertilizers application. Values represent means ± SEM (n = 3) for control and fertilization treatments. *p < 0.05, **p < 0.01, and ***p < 0.001.

Fig. 2. Response of various extractable biomarkers to mineral fertilizers application compared to control, of the bulk soil, particulate organic matter (POM), and mineral-associated organic matter (MAOM) fractions. Bars indicate differences in biomarkers concentration between the control and fertilization treatments. Positive values indicate increased concentration and negative values indicate decreased concentration compared to control.

Fig. 3. Response of bacterial, fungal, and their microbial residual carbon (MRC) contribution to soil organic carbon (SOC) accumulation in the particulate organic matter (POM) and mineral-associated organic matter (MAOM) fractions as influenced by mineral fertilizer application. Values represent means ± SEM (n = 3) for control and fertilization treatments. *p < 0.05, **p < 0.01, and ***p < 0.001.

Fig. 4. Biplots of principal component analysis (PCA) between compounds and related degradation proxies. Numbers in parenthesis represent data variations explained by first two principal components (PCs). ACL_{Alk}: average chain length of *n*-alkanes; ACL_{Fa}: average chain length of *n*-alkanoic acids; OEP: odd-over-even predominance of *n*-alkanes; EOP: even-over-odd predominance of *n*-alkanoic acids; ω-C_{16}/ΣC_{16}: C_{16} ω-hydroxy-alkanoic acids to all hydrolysable C_{16} aliphatic lipids; ω-C_{18}/ΣC_{18}: C_{18} ω-hydroxy-alkanoic acids to all hydrolysable C_{18} aliphatic lipids; Σmid/ΣS^C: the ratio of mid-chain-substituted hydroxy and epoxy acids to total cutin- and suberin-derived compounds; $(Ad/Al)_S$: the ratio of acid to aldehyde for syringyls; $(Ad/Al)_V$: the ratio of acid to aldehyde for vanillyls; VSC: total lignin-derived phenols; AS: total amino sugars; Fungal MRC: fungal microbial residual carbon; Bacterial MRC: bacterial microbial residual carbon

Fig. 5. Contributions of plant- (quantified as lignin), bacterial-, and fungal-derived carbon to soil organic carbon (SOC) in corresponding fractions.